Literature Report

Reporter: 许宁

Date: 2021-05-20

Article

Distinct fission signatures predict mitochondrial degradation or biogenesis

https://doi.org/10.1038/s41586-021-03510-6

Received: 15 November 2019

Accepted: 31 March 2021

Tatjana Kleele[1]✉, Timo Rey[1], Julius Winter[1], Sofia Zaganelli[1], Dora Mahecic[1], Hélène Perreten Lambert[1], Francesco Paolo Ruberto[2], Mohamed Nemir[2], Timothy Wai[3], Thierry Pedrazzini[2] & Suliana Manley[1]✉

Postdoctoral Researcher
Laboratory of Experimental Biophysics

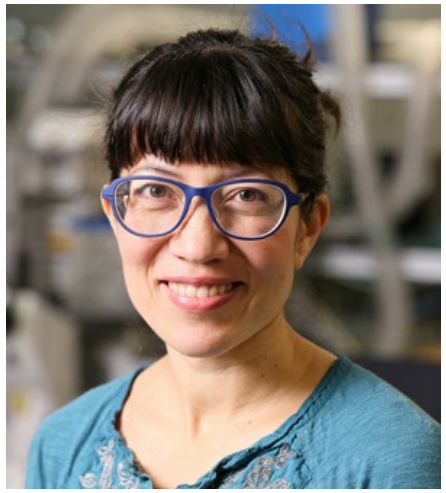

1997 B.A. Physics and Mathematics, Rice University
2004 PhD Physics, Harvard University.
2004-2006 Postdoctoral fellow, Department of Chemical Engineering, MIT, Cambridge, MA
2006-2009 National Research Council postdoctoral fellow, NICHD, NIH, Bethesda, MD
2009-2016 Assistant professor, Department of Physics, EPFL, Lausanne, Switzerland
2016-present Associate professor, Department of Physics, EPFL, Lausanne, Switzerland

Laboratory of Experimental Biophysics

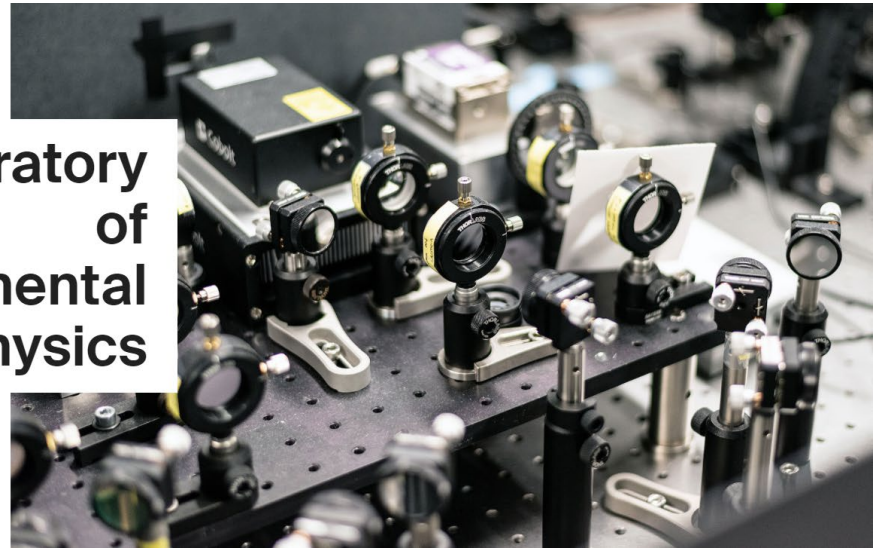

We develop and use automated super-resolution fluorescence imaging techniques combined with **live cell imaging** and **single molecule tracking** to determine how the dynamics of protein assembly are coordinated.

Large field-of-view super-resolution microscopy

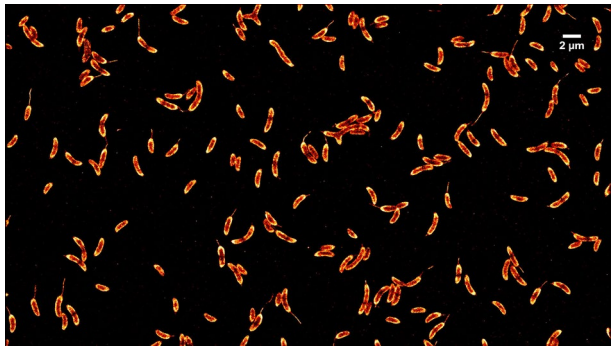

a large sample area (~150×150 µm^2)

Mitochondrial dynamics

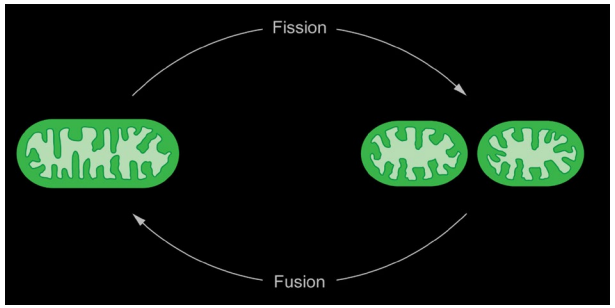

Organization of mitochondrial gene expression

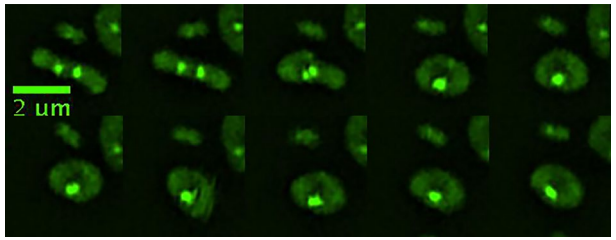

Multicolor 3D single particle reconstruction

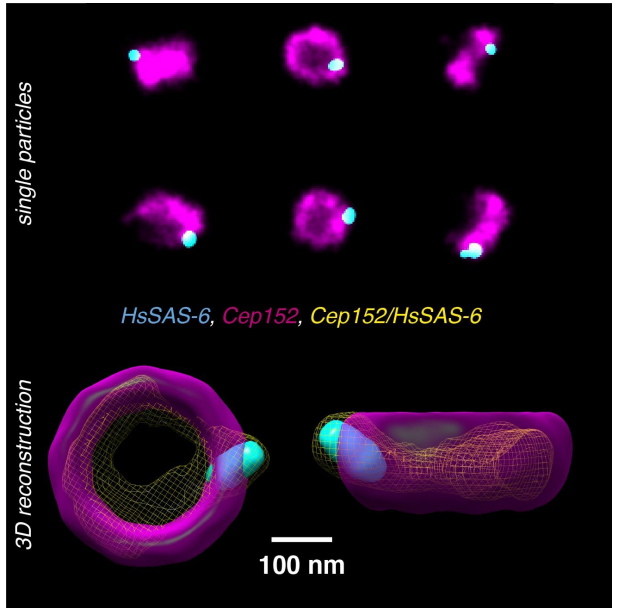

Waveguide TIRF for high-throughput DNA-PAINT

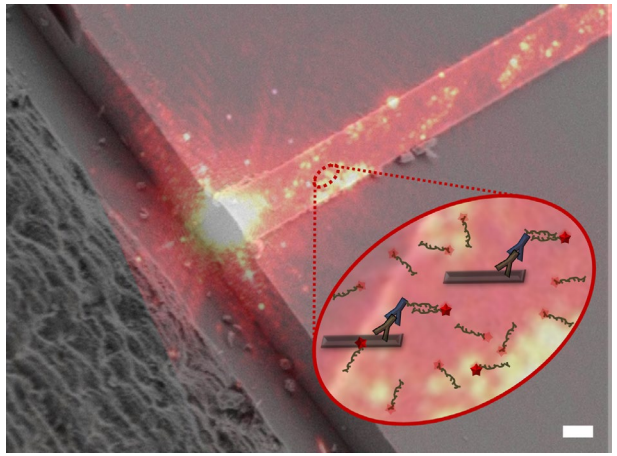

Cellular and physiological importance of the mitochondrial divisome.

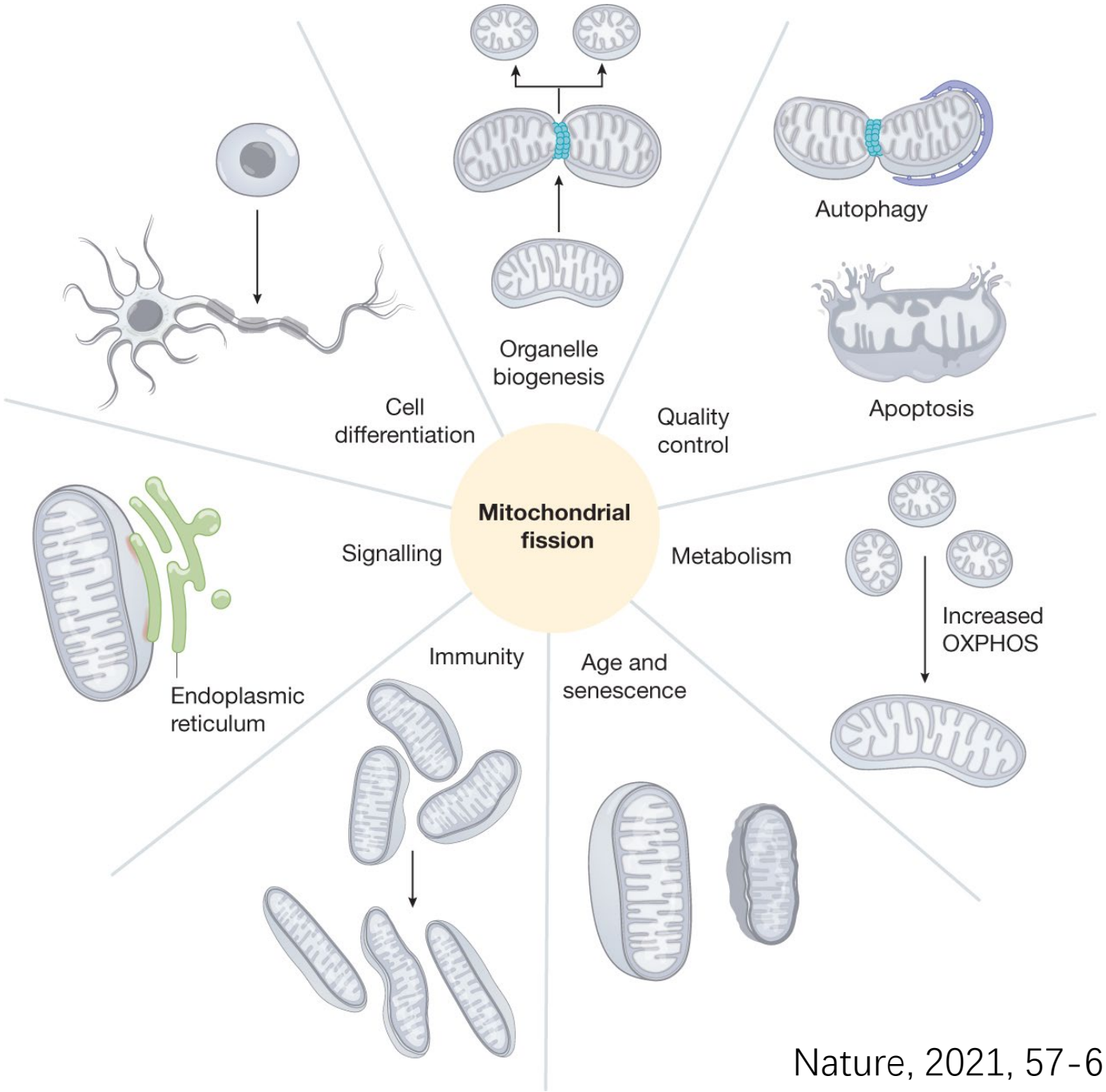

线粒体分裂失调:

神经退行性疾病
心血管疾病
癌症

Nature, 2021, 57-66.

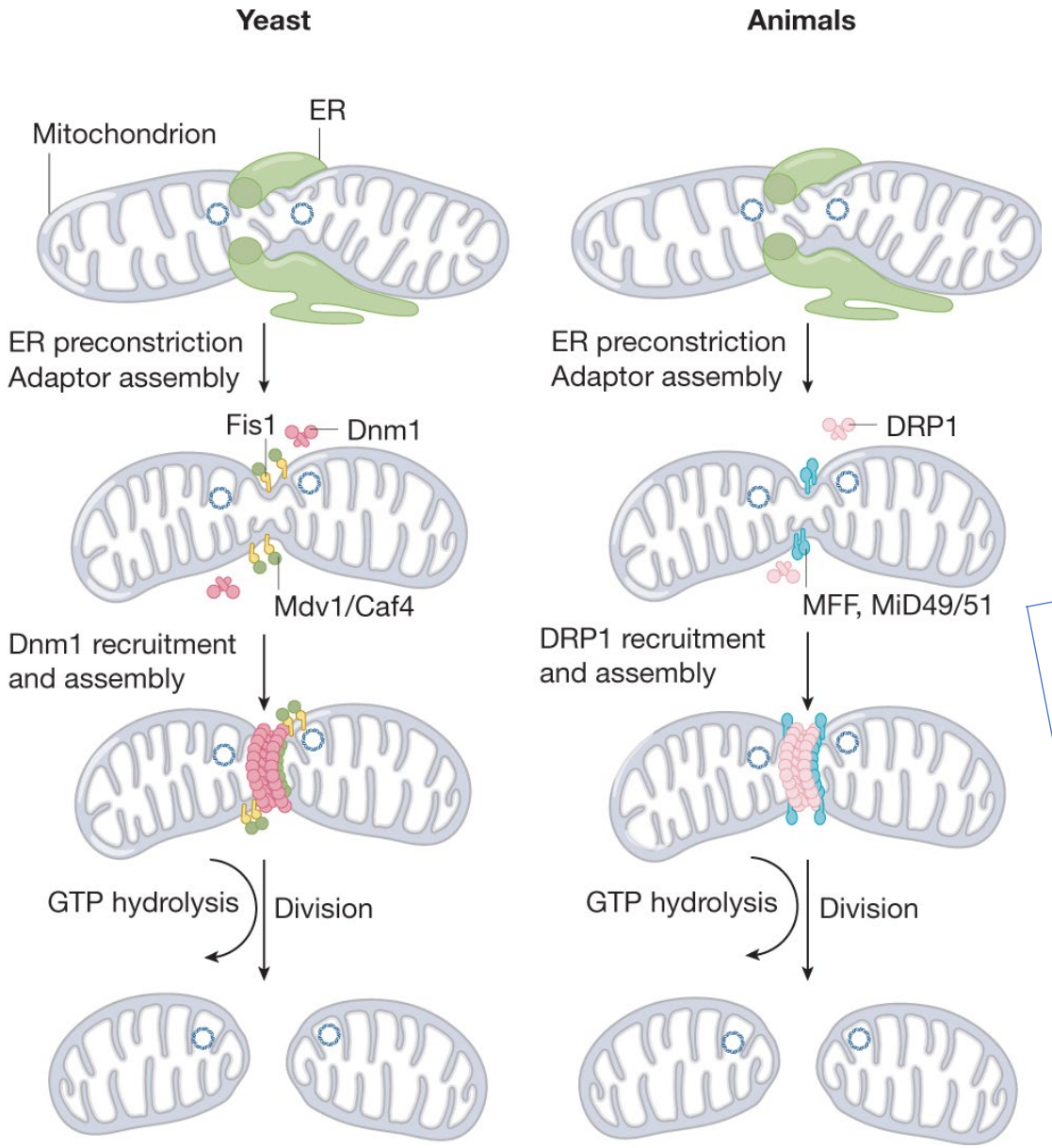

Nature, 2021, 57-66.

the GTPase of the dynamin superfamily of proteins
动力蛋白相关蛋白1（DRP1）

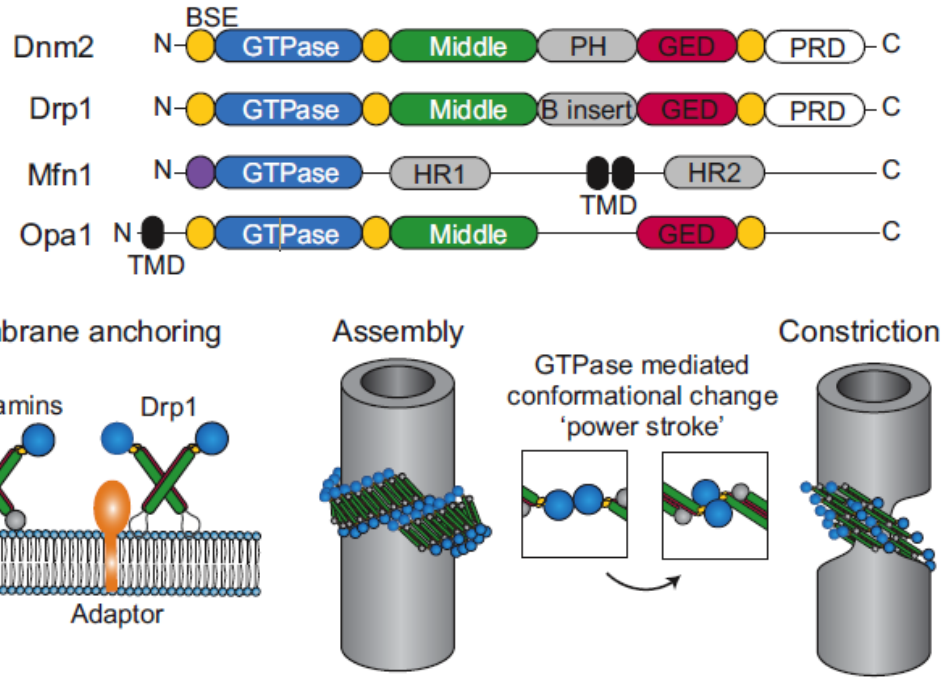

Journal of Cell Science, 2017, 1-8.

Distinct fission signatures predict mitochondrial degradation or biogenesis

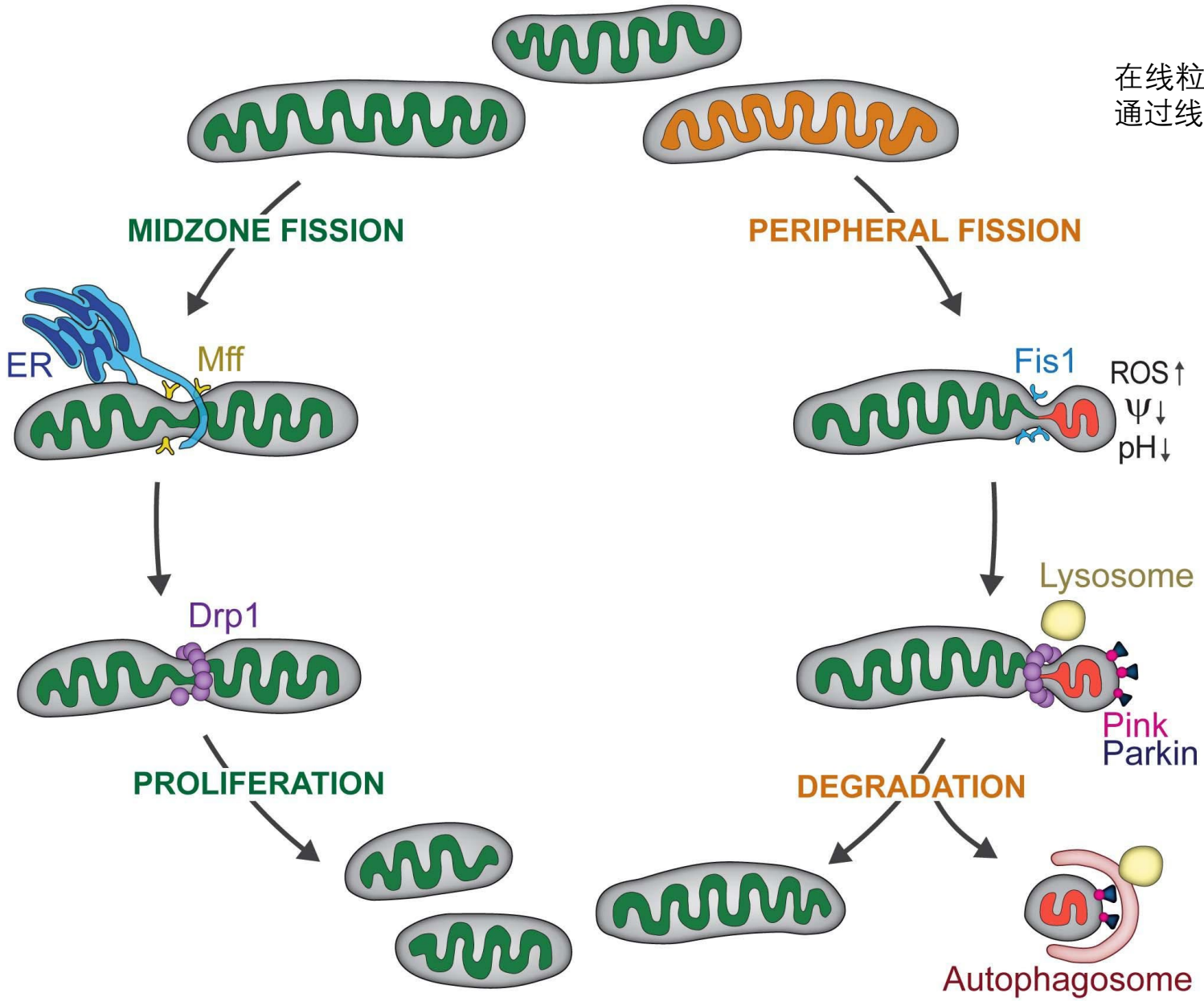

在线粒体的生命周期中，分裂既能使新的线粒体产生，又能通过线粒体自噬作用清除功能失调的线粒体。

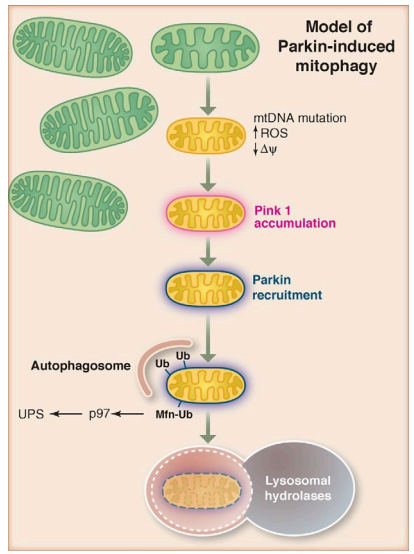

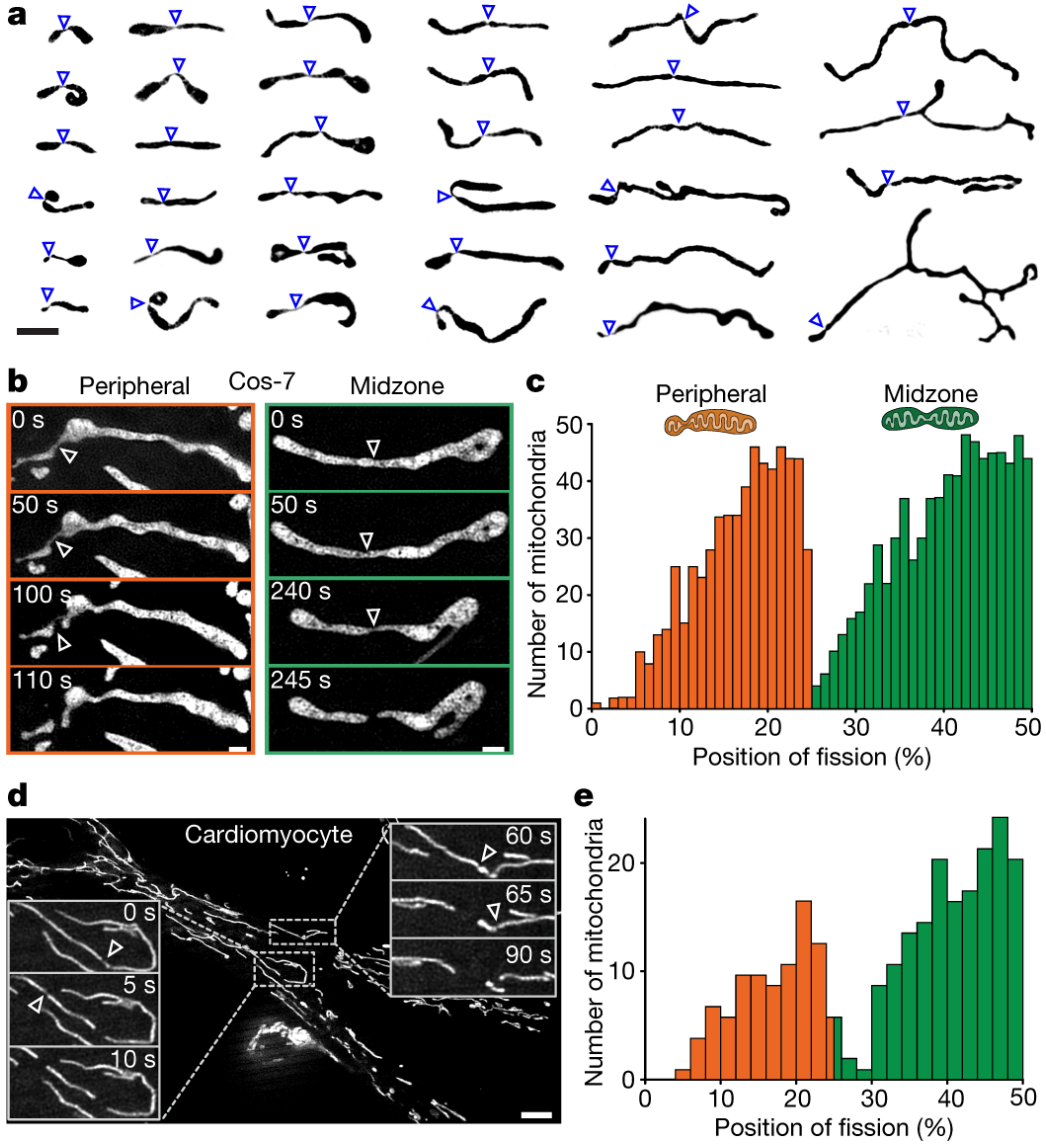

Peripheral divisions (less than 25% from a tip)

Midzone divisions (within the central 50%)

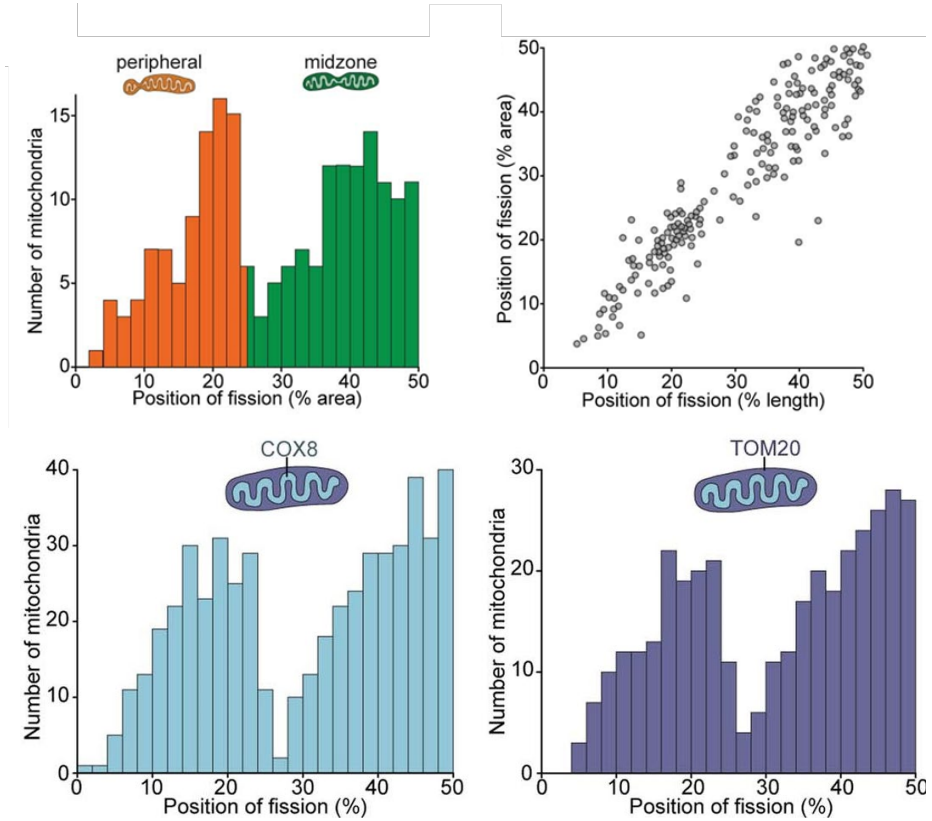

Fig. 1: Mitochondrial fissions are bimodally positioned and linked to distinct physiologies. a, Gallery of mitochondria one frame before division from structured illumination microscopy (SIM) movies, binarized. **b**, Time-lapse SIM sequence of a peripheral and a midzone fission of mitochondria (Mitotracker Green). **c**, Histogram of fission positions relative to the total mitochondrial length (n = 1,393 fissions pooled from multiple datasets). Fissions occurring near the tip (orange, 0–25%) are termed 'peripheral'; those near the centre (green, 25–50%) are termed 'midzone'. **d**, Instant SIM (iSIM) of mitochondria (Mitotracker Green) in primary mouse cardiomyocytes. Insets: time-lapse sequences from indicated boxes. , Histogram of the relative position of fission in cardiomyocyte mitochondria (n = 381 fissions), as in **c**.

Dysfunction precedes peripheral fission

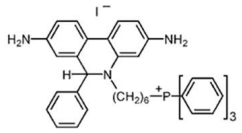

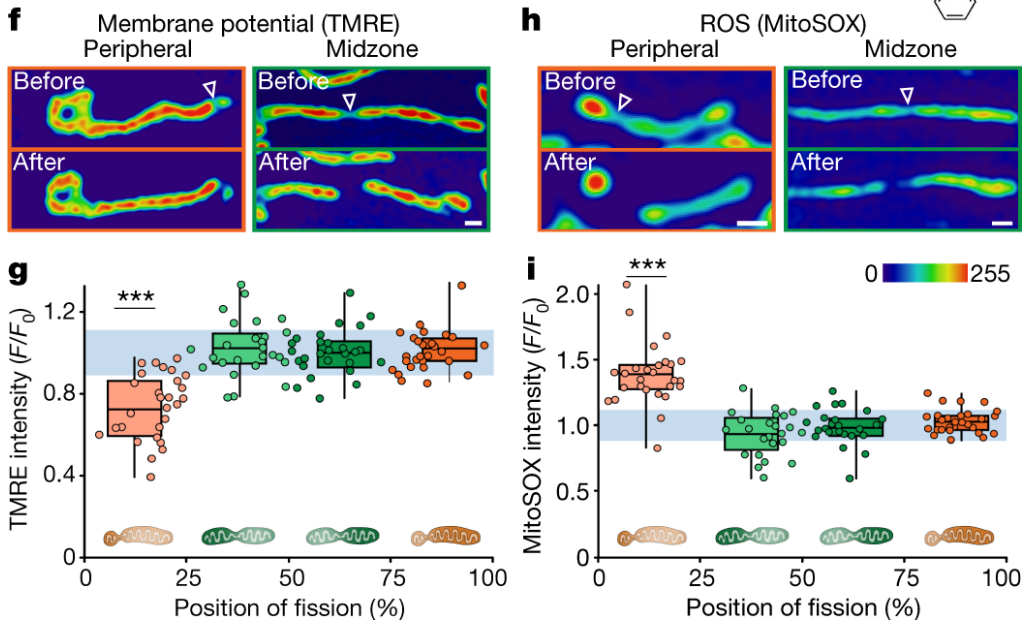

Fig. 1: Mitochondrial fissions are bimodally positioned and linked to distinct physiologies. **f**, Mitochondrial membrane potential before and after a peripheral or midzone fission from SIM movies of tetramethylrhodamine ethyl ester (TMRE)-stained mitochondria. **g**, Normalized TMRE intensity as a function of relative position of fission, measured immediately before fission (*n* = 56 fissions). **h**, MitoSOX labelling reveals ROS levels before and after a peripheral or midzone fission. **i**, Normalized MitoSOX intensity as a function of relative fission position, measured immediately before fission (*n* = 52 fissions).

几何上不同的分裂类型是否反映了潜在的生理差异

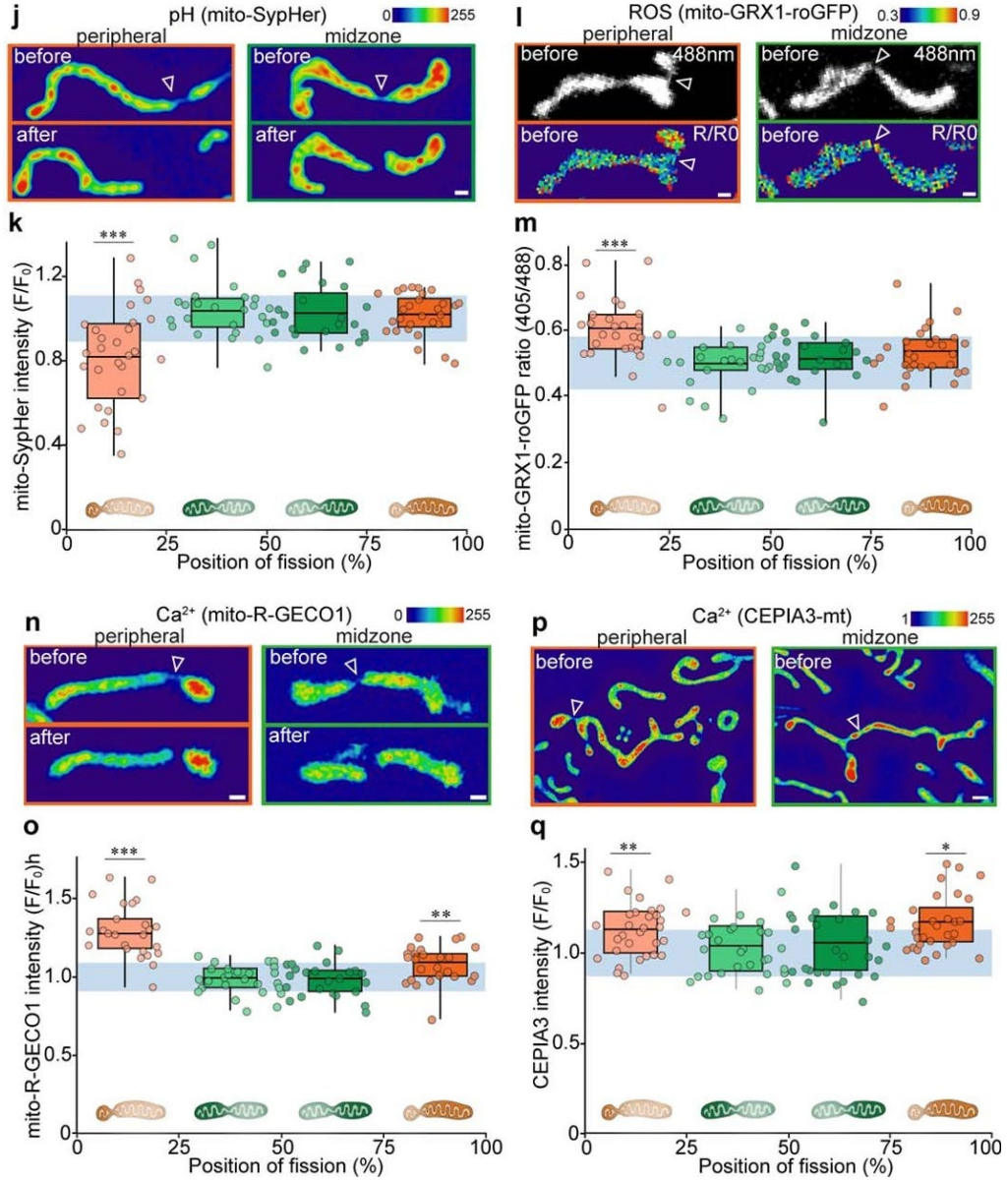

Midzone divisions
分裂前后的生理状态没有差异

Peripheral divisions
分裂前：Ca^{2+}和ROS浓度增加，膜电位和pH降低

Peripheral divisions → **degradation** Midzone divisions → **biogenesis** ?

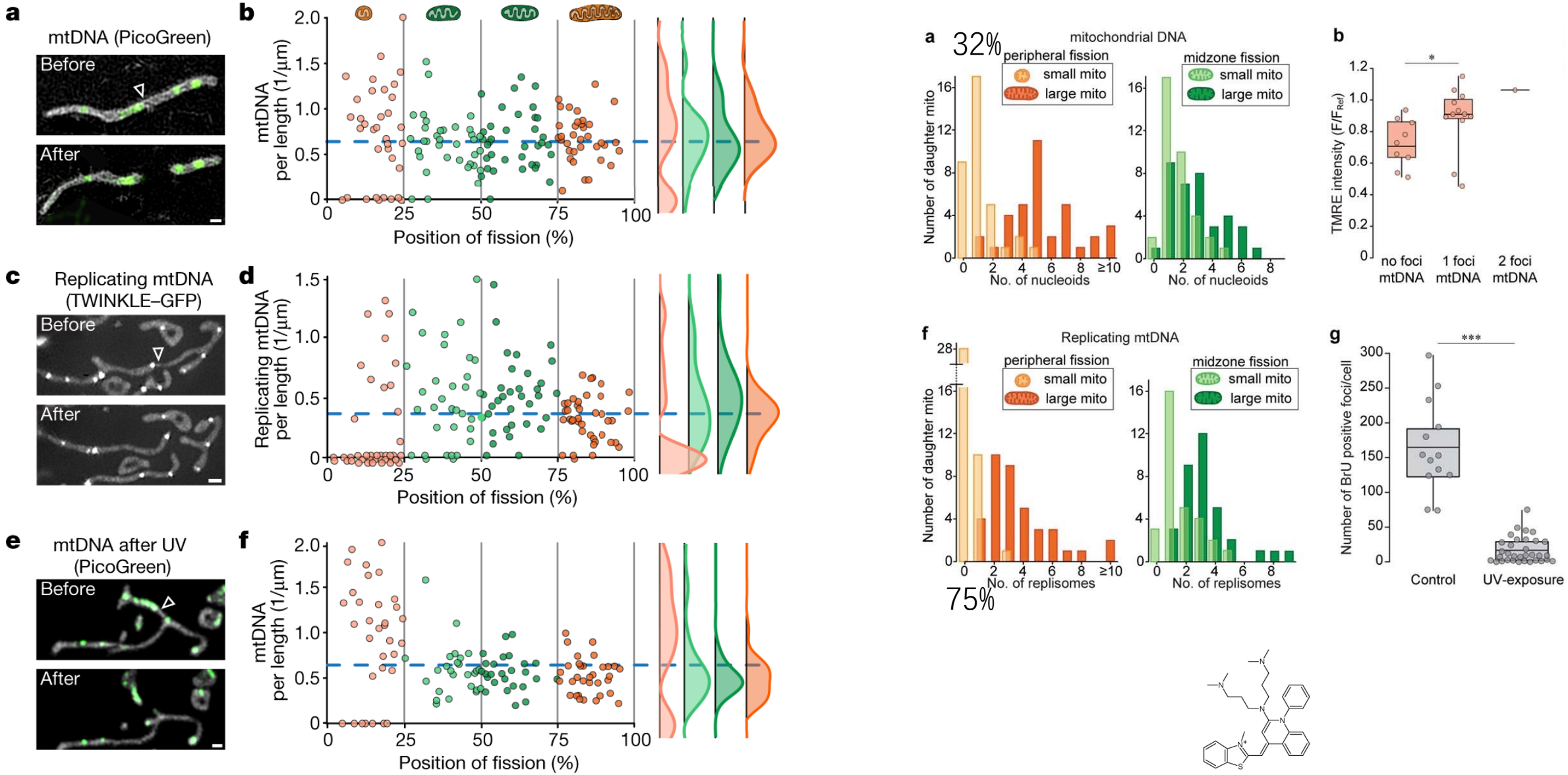

Fig. 2: Midzone and peripheral fissions differ in mitochondrial DNA content and fates. **a**, Mitochondria (mito–RFP) and mitochondrial (mt)DNA (PicoGreen, green) before and after fission. **b**, Linear density of nucleoids as a function of fission position, individual data points (left) and violin plots (right) for binned groups (*n* = 78 fissions). **c**, **d**, Replicating nucleoids (TWINKLE–GFP) (**c**) and linear density (**d**), as in **b** (*n* = 74 fissions). **e**, **f**, mtDNA (**e**) and linear density (**f**) after UV irradiation, as in **b** (*n* = 62 fissions).

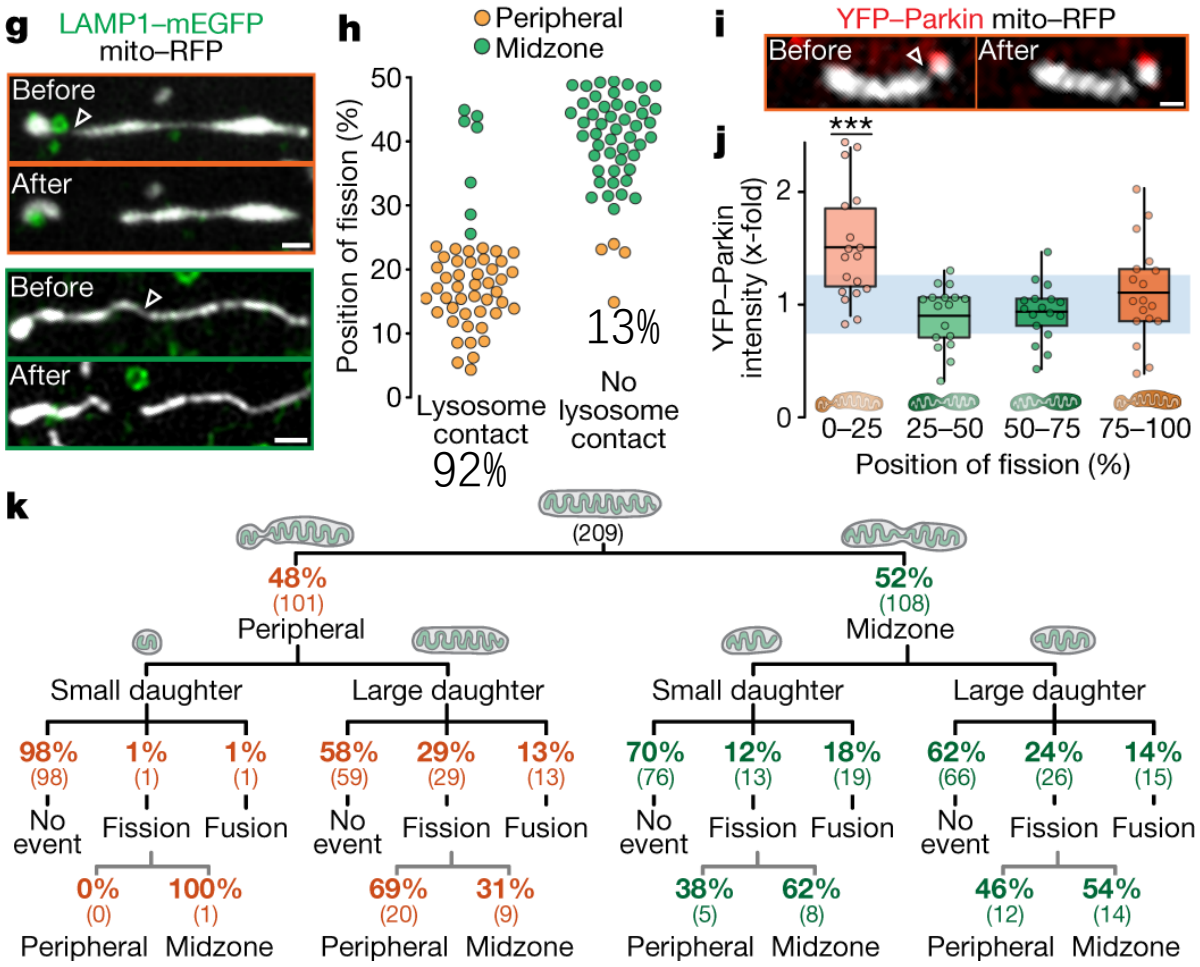

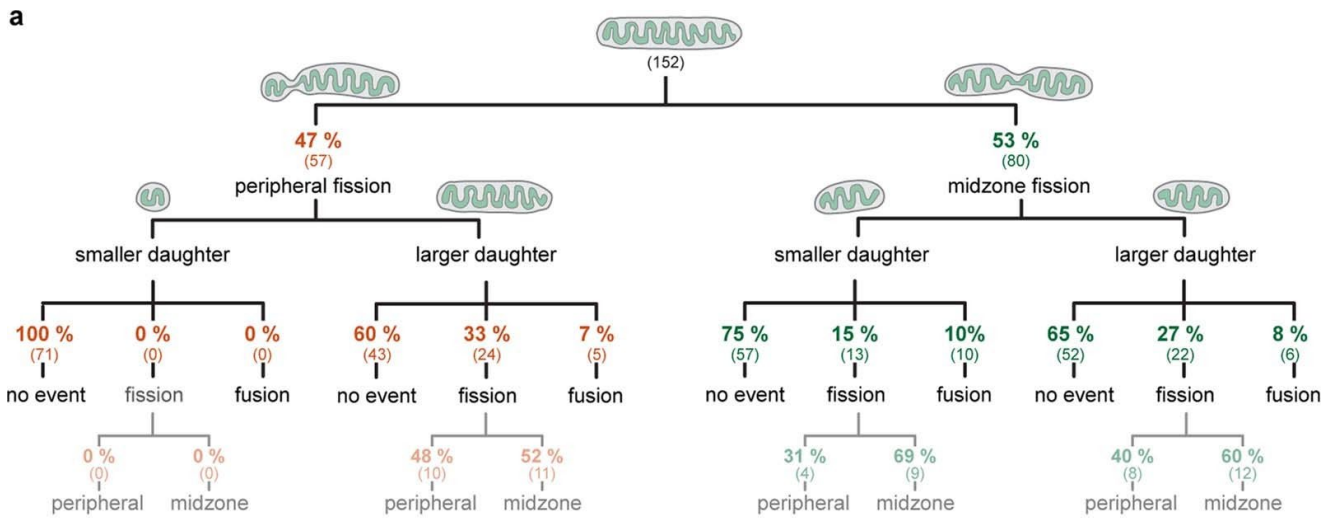

Fig. 2: Midzone and peripheral fissions differ in mitochondrial DNA content and fates. **g**, Mitochondria (mito–RFP, greyscale) and lysosomes (LAMP1–mEGFP, green) before and after peripheral or midzone fission. **h**, Position of fission in divisions contacting lysosomes or not before fission (*n* = 104 fissions). **i**, Mitochondria (mito–RFP, greyscale) and pre-mitophagic marker (YFP–Parkin, red) before and after fission. **j**, Pre-fission YFP–Parkin fold-change in intensity as a function of fission position (*n* = 34). **k**, Schema depicting the fates of daughter mitochondria from peripheral and midzone fissions. Mitochondria tracked for >100 s after fission were included. Numbers in parentheses are total numbers of events.

Changes in mitochondrial physiology and recruitment of the fission and autophagic machinery

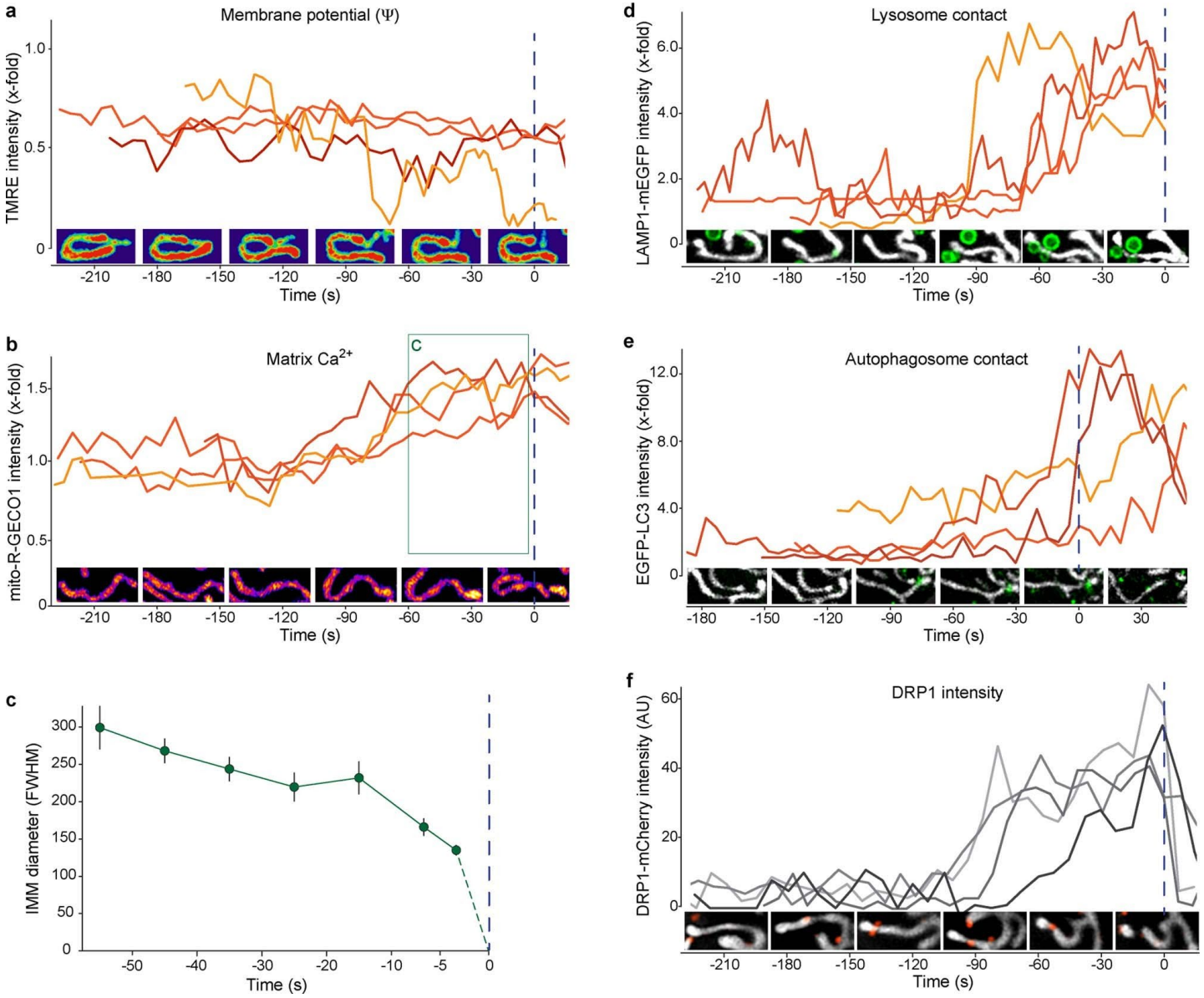

Fig. Time course of physiological changes and recruitment of fission regulatorsa, **b**, Time course of fluorescent signals in four examples of Cos-7 mitochondria displaying normalized TMRE intensity (**a**) and mito–R-GECO1 intensity (**b**) with corresponding SIM images in the mitochondrial compartment giving rise to the smaller daughter mitochondria before a peripheral division. **c**, Average inner membrane diameter at the constriction site at several time points before fission, measured in mito–R-GECO1 transfected Cos-7 cells during the time window where Ca^{2+} is elevated (green box in **b**, n = 10 fission events). **d**, **e**, Time course of lysosome co-localization (**d**) and autophagosome co-localization (**e**) at constriction sites for peripheral fissions, by measuring LAMP1−mEGFP and EGFP−LC3 intensity, respectively. For EGFP−LC3 measurements, cells were pre-treated with 10 µM CCCP to increase LC3 signals. **f**, Normalized DRP1 intensity at the constriction sites before peripheral fission in four examples of Cos-7 mitochondria with corresponding SIM images. Blue dotted lines (t = 0 s) mark the time point of fission.

Cell context-dependent modulation

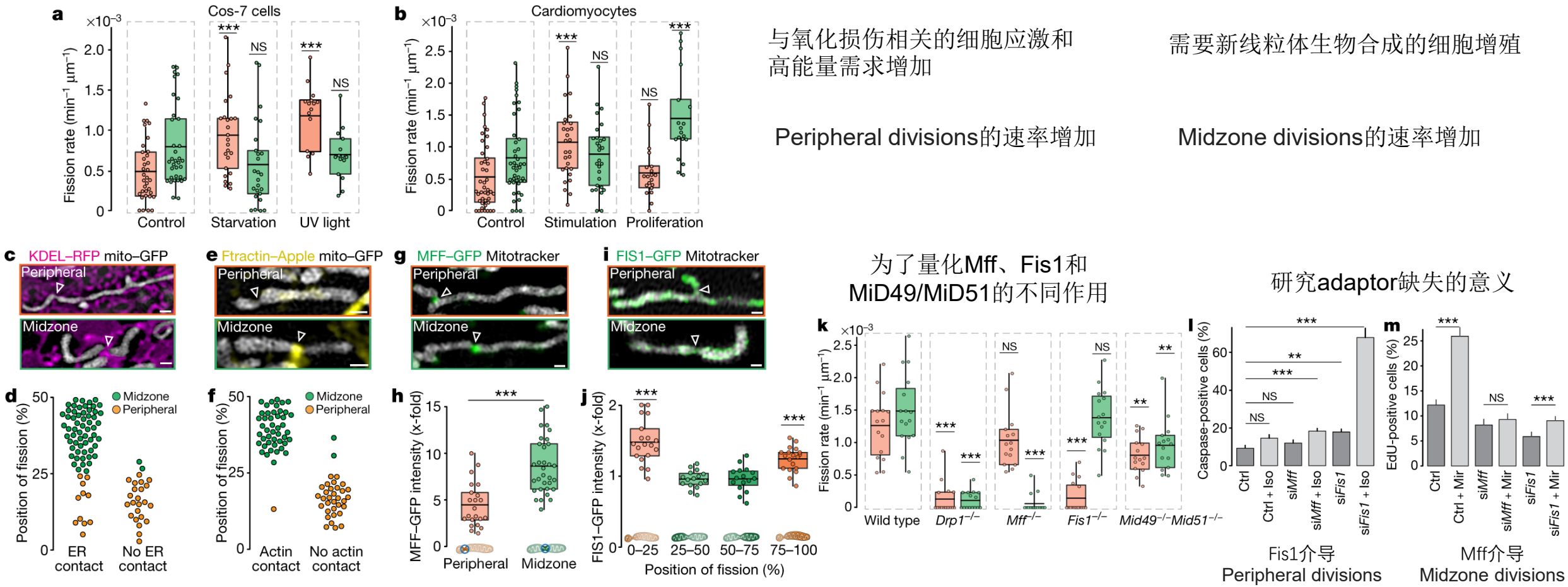

与氧化损伤相关的细胞应激和高能量需求增加

Peripheral divisions的速率增加

需要新线粒体生物合成的细胞增殖

Midzone divisions的速率增加

为了量化Mff、Fis1和MiD49/MiD51的不同作用

研究adaptor缺失的意义

Fis1介导 Peripheral divisions

Mff介导 Midzone divisions

Fig. 3: Midzone and peripheral fissions are independently regulated by distinct molecular machineries. **a**, Peripheral (orange) and midzone (green) fission rates in control, starved or UV-exposed Cos-7 cells ($n \geq 15$ fields of view (FOV) per group). **b**, Fission rates in postnatal mouse cardiomyocytes in control, stimulated or proliferation-induced cells ($n \geq 19$ FOV per group). **c**, SIM of mitochondria (mito–GFP, grey) and endoplasmic reticulum (ER) (KDEL–RFP, magenta) before a peripheral or midzone fission. **d**, Position of fission in mitochondria contacting the ER (left) or not (right) before fission ($n = 93$ fissions) in Cos-7 cells. **e**, SIM of mitochondria (mito–GFP, grey) and actin (Ftractin–Apple, yellow) before peripheral and midzone fissions. **f**, Fission position in mitochondria that accumulate actin (left) or not (right) before fission ($n = 80$ fissions). **g**, SIM of mitochondria (Mitotracker Red, grey) in U2OS cells endogenously expressing MFF–GFP for a peripheral and a midzone fission. **h**, MFF–GFP fold-change in intensity at the fission site of peripheral and midzone divisions ($n = 54$ fissions). **i**, SIM of mitochondria (Mitotracker Red, grey) in U2OS cells endogenously expressing FIS1–GFP (green) for a peripheral and a midzone fission. **j**, FIS1–GFP fold-change in intensity over the surface of a daughter mitochondrion before fission ($n = 35$ fissions). **k**, Peripheral (orange) and midzone (green) fission rates in wild-type, *Drp1*$^{-/-}$, *Mff*$^{-/-}$, *Fis1*$^{-/-}$ and *Mid49*$^{-/-}$*Mid51*$^{-/-}$ double-knockout mouse embryonic fibroblasts, stained with Mitotracker Green ($n \geq 15$ cells per group). **l**, Percentage of apoptotic (caspase 3/caspase 7-positive) cardiomyocytes (± s.e.m.) in control, FIS1- and MFF-depleted cells with or without stimulation with isoproterenol ($n > 29$ FOV per group). **m**, Percentage of proliferating (EdU-positive) cardiomyocytes (± s.e.m.) in control, FIS1- and MFF-depleted cells with or without treatment with miR-199 (Mir) ($n \geq 49$ FOV per group).